JOURNAL OF MATERIALS SCIENCE 27 (1992) 4890–4898

Influence of ethanol washing of the hydrous precursor on the textural and structural properties of zirconia

P. D. L. MERCERA*, J. G. VAN OMMEN, E. B. M. DOESBURG, A. J. BURGGRAAF, J. R. H. ROSS‡
Laboratory of Inorganic Chemistry, Materials Science and Catalysis, Faculty of Chemical Technology, University of Twente, PO Box 217, 7500AE Enschede, The Netherlands

The influence of post-precipitation washing with ethanol on the evolution of the porous texture and structure of ZrO_2 upon calcination in air has been investigated. Washing of the hydrogel of zirconia with ethanol was found to exert little influence on the process of crystallization of the hydrous zirconia: neither the temperature of crystallization nor the enthalpy change associated with the transition of the amorphous to the metastable tetragonal phase of zirconia was influenced significantly. On the other hand, the thermal stability of the tetragonal phase formed was found to be drastically reduced by effects imparted by the nature of the solvent used for washing the hydrogel; the process of phase-transformation to the thermodynamically more stable monoclinic modification was promoted strongly as a consequence of the washing with ethanol. This influence of ethanol washing appears to arise from a promotional effect of carbonaceous residues; these carbonaceous impurities are thought to facilitate the nucleation of the monoclinic phase. Washing the precipitate with ethanol was also found to have a profound effect on the textural properties of the (calcined) zirconia: the specific surface area, total pore volume and most frequent pore radius were all increased significantly. These effects of ethanol washing are believed to be due to an inhibition of polycondensation reactions of the surface hydroxyl groups located on adjacent particles which would have yielded new Zr–O–Zr bonds; this is probably associated with the presence of surface ethoxide species, the formation of which has been shown.

1. Introduction

Zirconium dioxide is currently attracting considerable interest as support material in a variety of catalyst systems. In most of the cases, this interest can be ascribed to at least one of the following three properties of zirconia: (i) as a carrier, it gives rise to a unique kind of interaction between the active phase and support, this being manifested in both the catalytic activity and selectivity pattern of the system [1–6]; (ii) it is more chemically inert than the classical supports (e.g. γ-Al_2O_3 or SiO_2) [7, 8]; and (iii) it is the only single-metal oxide which may possess four chemical properties, namely acidity or basicity as well as reducing or oxidizing ability [9].

It has become well established that the performance of a heterogeneous catalyst not only depends on the intrinsic catalytic activity of the constituents but also on its texture and stability. One of the most important factors in controlling the texture and strength of a catalyst involves the correct choice of a support and the preparation of the support in the appropriate form [10, 11]. Many industrial applications require supports which combine a high specific surface area with good thermal and chemical stabilities. Furthermore, the internal surface area of the support must be easily accessible to the reactants, a requirement which implies that the pores must not be too narrow. According to Trimm [11], the most frequent pore radius must preferably be larger than 5 nm. Thus, for most applications, the catalyst support material must possess a well-developed mesoporous texture.

In a previous paper [12], we have shown that mesoporous zirconium dioxide with a high specific surface area (S_{BET} = 111 $m^2 g^{-1}$) could be made by gel precipitation followed by calcination at 450 °C. However, the total specific pore volume was low (V_p = 0.11 $cm^3 g^{-1}$) and, more importantly, the internal surface area was found to be contained mainly within narrow mesopores, the most frequent pore radius being about 2.1 nm. Moreover, approximately 9% total pore volume was established to be micropore volume (i.e. consisting of pores with radii smaller than about 1 nm [13]) and the area determined from t-plots (the sum of the areas of the mesopore walls and the external surface) was 89 $m^2 g^{-1}$. (Because of the presence of microporosity, the latter value has more physical significance than the area calculated by the BET method.)

* Author to whom all correspondence should be addressed.
‡ *Present address*: Department of Industrial Chemistry and Chemical Engineering, University of Limerick, Plassey Park, Limerick, Ireland.

0022–2461

Mesoporosity arises mainly from voids between entities; these voids may be between the (primary) crystallites which make up the agglomerates (the so-called "intra-agglomerate pores") or between the agglomerates constituting the larger aggregates (the so-called "inter-agglomerate pores"). Important factors influencing the degree of mesoporosity and the total pore volume of zirconium dioxide prepared via wet-chemical routes include the pH of precipitation and the method of dehydration of the hydrogel. The degree of mesoporosity as well as the total pore volume have been found to increase with increasing pH [12, 14–16]; in our laboratory, the precipitation of hydrous zirconia is normally carried out at an optimum pH of 10 [12]. Dehydration of the hydrogel of zirconia by drying at temperatures in the range 80–130 °C brings about a marked contraction of the gel, the resulting xerogel being dense and glass-like [12, 14, 17, 18]. The influence of drying of the hydrogel of zirconia on the textural properties of the resulting xerogel is represented schematically in Fig. 1. This figure illustrates the relationship between pore volume, V_p, and the surface area of the crystallites, S_{cryst}, for pores of cylindrical geometry as a hydrogel is dried to a xerogel: "A" represents the texturally poorly defined hydrogel, while "B" represents the resultant dried gel. The pore radius is given by $2V_p/S_{cryst}$ or twice the gradient of the lines shown. (It is assumed that no hydrothermal ageing occurs during the drying of the hydrogel; the occurrence of hydrothermal ageing may give rise to a coarsening of the crystallites thus leading to a decrease in S_{cryst}.) Clearly, the degree of mesoporosity will be markedly influenced by the process of dehydration of the hydrous zirconia. Consequently, any treatment of the hydrogel which brings about less collapse of the porous texture upon formation of the xerogel will result in an increase in the mean pore radius and thus in an increase in the degree of mesoporosity.

The contraction of the structure of the hydrogel of zirconia upon drying to yield hard and dense agglomerates is a well documented phenomenon in the ceramic literature and the mechanisms proposed to account for its occurrence include the action of capillary forces [19–21] and/or condensation reactions

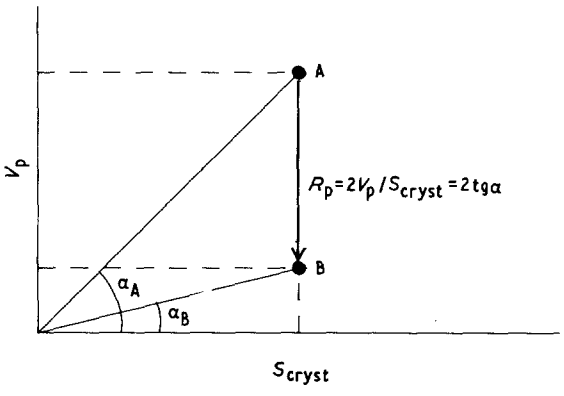

Figure 1 Relationship between pore volume, V_p, crystallite surface area, S_{cryst}, and mean pore radius, R_p, as a hydrogel is dried to a xerogel: A, the texturally poorly defined hydrogel; B, the resultant dried gel.

involving surface hydroxyl groups located on adjacent particles to yield new Zr–O–Zr bonds [18, 22, 23]. Various ways of treating the hydrogel to reduce the incidence of hard agglomerates and to increase the porosity of the xerogel have been described among which are freeze-drying [20, 21] and washing with organic liquids [17, 19, 24]; the latter method is the most commonly used technique, the liquids normally employed being alcohols. Although the influence of alcohol washing on the morphology of zirconia powders has been investigated extensively [17, 18, 22–24], little attention has been paid to the use of alcohols in regulating the textural and structural properties of zirconia. Sheinfain and Makovskaya [19] have carried out a fairly systematic study of the influence of organic liquids on the development of the porous texture of hydrous zirconia, but they did not investigate the influence of post-precipitation washing on the evolution of the crystal structure of ZrO_2. The present investigation thus sets out to study the influence of post-precipitation washing with ethanol on the evolution of the porous texture and structure of ZrO_2 upon calcination in air.

2. Experimental procedure

2.1. Preparation of the samples

Samples of hydrous zirconia were made by controlled precipitation at room temperature. A solution of zirconyl chloride (0.4 M) was added dropwise, at a rate of 10 $cm^3\ min^{-1}$, concurrently with a solution of ammonia (6.7 M) to doubly distilled water, the pH of which had been adjusted to 10 with ammonia; the pH was maintained at 10 by adjusting the rate of addition of the ammonia solution. The whitish gelatinous precipitate formed was aged in the mother liquor for 65 h; after filtration, it was washed in a sequence of repeated cycles involving redispersion in doubly distilled water and filtration until the wash-water gave a negative test for chloride ions (addition of a 3 M $AgNO_3$ solution).

To investigate the effects of washing, the Cl^--free hydrogel was separated into two batches. One batch was further subjected to two cycles involving redispersion in doubly distilled water and filtration (sample ZrW); the other batch was subjected to two cycles involving redispersion in ethanol (purity 99.8%) and filtration (sample ZrE). The precipitation and redispersion steps were carried out in the reactor described previously [12, 25]. After the last dispersion steps, the gels were dried in static air at 110 °C for 20 h; ZrW was hard and glass-like while ZrE was soft and friable. The dried gel ZrW was ground to particle sizes of less than 100 μm using an agate pestle and mortar; the xerogel of ZrE was dry-milled in a plastic container employing teflon balls to yield a fluffy white powder.

2.2. Chemical analysis

The purity of the samples ZrW and ZrE was determined using X-ray fluorescence analysis (XRF, Philips PW 1410 spectrometer). The bulk chloride content, which serves also as a quality control parameter, was

determined quantitatively by an argentometric method, the details of which were given previously [12].

2.3. Calcination procedure

The samples were studied both in the freshly prepared state and after calcination. Calcination was carried out in a flow of air (150 $cm^3 min^{-1}$) in a tube furnace at various temperatures up to 850 °C. The temperature was increased at a rate of 3 °C min^{-1} to the final temperature; this was maintained for 15 h before the sample was cooled to 200 °C at a rate of 5 °C min^{-1}, after which it was cooled rapidly to room temperature.

2.4. Characterization techniques

The fresh and calcined samples were characterized by thermogravimetry (TG), differential scanning calorimetry (DSC), nitrogen physisorption measurements, Raman spectroscopy and X-ray powder diffraction (XRD). The thermal analyses were all performed by raising the temperature linearly at a rate of 10 °C min^{-1} in a flow of air (35 $cm^3 min^{-1}$). The TG studies were carried out using a PL Thermal Sciences system (STA-1500), while the DSC studies were performed using a Stanton Redcroft apparatus (DSC 1500 system) together with a Stanton Redcroft high-sensitivity DSC cell. A sample of α-Al_2O_3 was used as reference for the DSC measurements.

Full nitrogen adsorption–desorption isotherms at −196 °C were measured for granules of the samples ZrW and ZrE using a Micromeritics ASAP 2400 system; to this end, portions of the calcined powder samples were pressed at 592 MPa, and then crushed and sieved to a particle size of 0.3–0.6 mm. Prior to the physisorption measurements, all the samples were outgassed for 6 h at 300 °C. Analysis of the isotherms was carried out as described previously [12].

Raman spectra of selected samples were obtained with a SPEX 1877 spectrometer equipped with an argon-ion laser (wavelength $\lambda = 533$ nm and power $W = 15$ mW).

X-ray diffraction patterns were recorded using a Philips PW 1710 diffractometer with nickel-filtered CuK_α radiation. Both continuous and step-scan techniques were used, the former being employed for phase identification and the latter for quantitative analysis. The step-scans were taken over the range of 2θ from 26°–33° in steps of 0.015° (2θ), the intensity data for each point being collected for 10 s. In order to improve counting statistics further, rotation about the normal axis was used. The collected data were analysed according to the procedure described previously [12]; this involved resolving the overlapping peaks by best-fitting the diffraction profiles using asymmetric Lorentzians. The volume fraction , V_m, of the monoclinic phase in the calcined samples was calculated from the integrated intensity ratio, X_m

$$X_m = \frac{I_m(1\,1\,-1) + I_m(1\,1\,1)}{I_m(1\,1\,-1) + I_m(1\,1\,1) + I_t(1\,1\,1)} \quad (1)$$

using the non-linear relationship proposed by Toraya *et al.* [26]

$$V_m = \frac{1.31 X_m}{1 + 0.31 X_m} \quad (2)$$

The subscripts m and t represent the monoclinic and the tetragonal phases, respectively.

3. Results and discussion

3.1. Chemical analysis

XRF analyses of the samples ZrW and ZrE revealed the presence of the following impurities: hafnium (major impurity), traces of copper, iron, titanium, potassium and silicon, together with some chlorine. The bulk chloride analyses showed that the two samples contained less than 50 p.p.m. chloride ions; 50 p.p.m. is approximately the detection limit of the method employed.

3.2. Influence of ethanol washing on the structural properties of zirconia

3.2.1. Freshly prepared samples: thermal analysis

The X-ray diffractograms of the uncalcined samples showed only very broad bands in the range of 2θ from 18°–40° and from 40°–70°, this being indicative of a very low degree of crystallinity. The lack of well-defined reflections in the XRD patterns of the xerogels is typical of that for zirconia prepared via wet-chemical routes [12, 23, 27].

Typical TG and DSC results of the decomposition of the ZrW xerogel are shown in Fig. 2. These results are very similar to those reported by us previously for a zirconia prepared by an analogous route [12]. The process of loss of weight due to the volatilization of water occurred in two stages and did not cease until a temperature of approximately 500 °C was attained (Fig. 2a); DSC (Fig. 2b) showed that these two weight losses were mildly endothermic. The final weight loss was about 19% of the initial sample weight. At about 445 °C, an intense and very sharp exothermic peak was observed (Fig. 2b). The enthalpy change associated with this so-called "glow-exotherm", characteristic of the crystallization of the initially (X-ray) amorphous hydrous zirconia, was estimated to be 20.5 kJ $(mol\,ZrO_2)^{-1}$. These results are also in good agreement with the findings of other investigators for similar zirconia systems [28, 29].

As shown in Fig. 3, the decomposition of the dried gel ZrE, on the other hand, occurred in four distinct stages, the rate of weight loss (DTG curve) achieving maxima at about 69, 193, 336 and 465 °C (Fig. 3a). Infrared studies of samples of ZrE at various stages of the decomposition [30] showed that the first two stages were due to the desorption of physically adsorbed water and the volatilization of water of crystallization, respectively; the third and fourth peak in the DTG trace corresponded to the oxidative decomposition of chemisorbed ethanolic species (i.e. surface ethoxide groups), a process which is likely to be ZrO_2-catalysed [18]. The formation of (surface) ethoxide

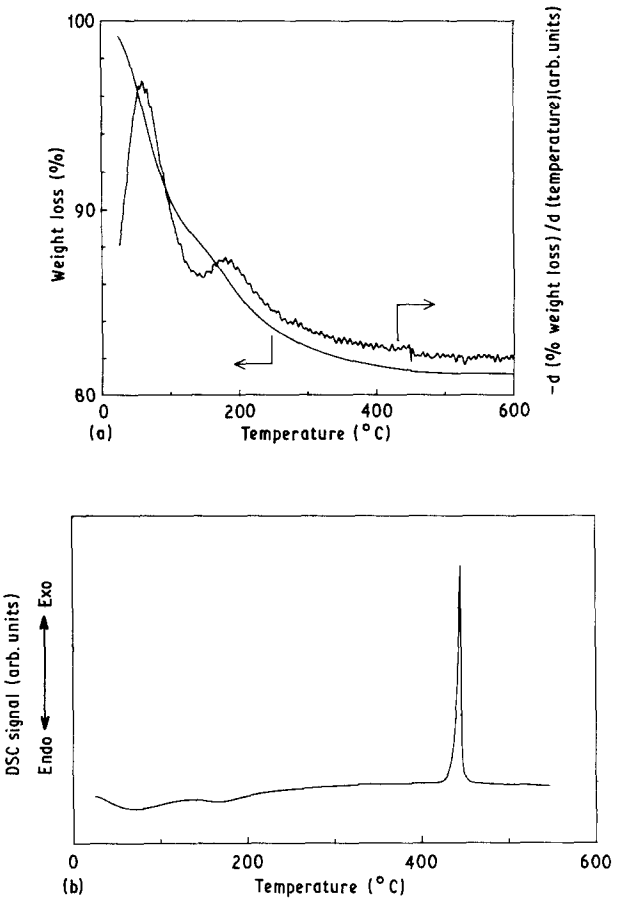

Figure 2 Thermal analysis results of the decomposition of the xerogel ZrW: (a) typical thermogravimetric analysis (TG) results; (b) typical differential scanning calorimetry (DSC) results.

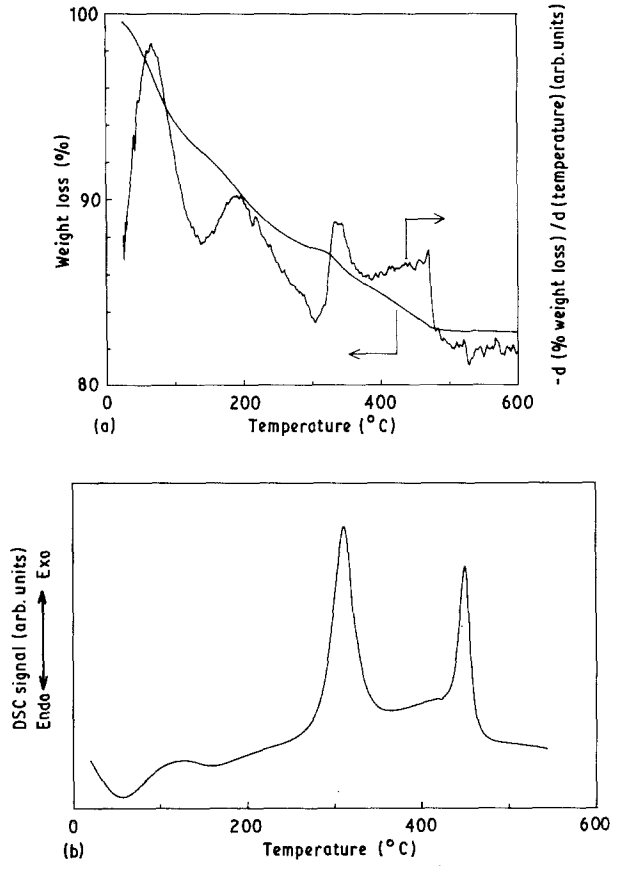

Figure 3 Thermal analysis results of the decomposition of the xerogel ZrE: (a) typical thermogravimetric analysis (TG) results; (b) typical differential scanning calorimetry (DSC) results.

groups during ethanol washing has also been reported by Kaliszewski and Heuer [18]. The loss of weight was complete at about 480 °C and was appoximately 17% of the initial sample weight. As shown in Fig. 3b, the first two weight losses were mildly endothermic, while the third was strongly exothermic (exotherm at about 310 °C). (It should be noted that the last weight loss, the DTG peak at about 465 °C (Fig. 3a), has been shown to be mildly exothermic [27].) The glow-exotherm (the last exotherm in Fig. 3b) occurred at about 450 °C and was significantly broadened compared to that of ZrW (Fig. 2b). The enthalpy change associated with the glow phenomenon was measured to be approximately 18.6 kJ (mol ZrO_2)$^{-1}$, which was very similar to the value determined for ZrW.

3.2.2. Crystallization and evolution of the structure on calcination

The samples ZrW and ZrE both crystallized on calcination at 450 °C in the (metastable) tetragonal phase of zirconia rather than into the thermodynamically more stable monoclinic phase; this was established by using X-ray powder diffraction (XRD) supplemented by Raman spectroscopy. Additional information from Raman scattering experiments was required because the X-ray reflections exhibited by the samples ZrW and ZrE after the process of crystallization were subjected to considerable broadening, making it impossible to distinguish clearly between the nearly identical X-ray patterns of the tetragonal and cubic polymorphs of ZrO_2. The Raman spectra of the various polymorphs of ZrO_2, on the other hand, are readily distinguishable and well-established from numerous experimental and theoretical studies [12, 28, 31–35]. A typical Raman spectrum of a sample of zirconia (ZrW) after crystallization at 450 °C is shown in Fig. 4. The Raman shifts, which are characteristic of the tetragonal symmetry of ZrO_2, are marked with asterisks; the unmarked peaks could be assigned to the strongest Raman shifts of the monoclinic phase of zirconia and were thus indicative of the presence of some of this phase.

The results of X-ray phase analyses for each of the samples calcined at various temperatures are shown in

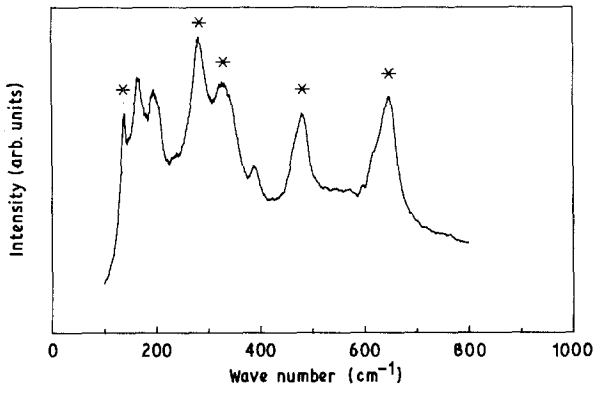

Figure 4 Typical Raman spectrum of a predominantly tetragonal zirconia sample obtained by heat treating hydrous zirconia at 450 °C to effect crystallization. (*) The bands which are characteristic of tetragonal symmetry.

Fig. 5, in which the volume fractions, V_m, of monoclinic phase are plotted against calcination temperature. It is clear that the "thermal stability" of the tetragonal phase was markedly influenced by effects imparted by the nature of the solvent used for washing the precipitate, the phase transformation to the thermodynamically more stable monoclinic phase being promoted strongly as a consequence of washing with ethanol.

3.2.3. Metastable tetragonal zirconia

The initial formation and "stability" of the (metastable) tetragonal phase has previously been rationalized in different ways, but the explanations still remain controversial. Livage *et al.* [36], Wu and Yu [37], and Blesa *et al.* [38] considered the initial formation of the tetragonal phase to be a consequence of the structural similarity between the amorphous and tetragonal forms of zirconia. Similarly, Tani *et al.* [39] proposed a mechanism of topotactic crystallization of tetragonal zirconia on nuclei in the amorphous ZrO_2. Cypres *et al.* [40] considered the stabilization to result from the effect of anionic "impurities" such as OH^- or SO_4^{2-}. Davis and co-workers [28, 41, 42] argued that the tetragonal phase was stabilized by chemical factors introduced during the precipitation process (e.g. by the pH), the associated hydroxyl concentration being the dominant factor. In yet another approach, Garvie and co-workers [43–45] and Pyun *et al.* [46] attributed the stabilization to surface- and strain-energy effects (this explanation being thermodynamic rather than kinetic); these effects allowed the calculation of a critical crystallite size below which the tetragonal phase was more stable than the monoclinic modification. Finally, Rijnten [14] and also Mitsuhashi *et al.* [47] rationalized the stabilization in terms of the effect of a strain energy generated at domain boundaries.

We have shown in a previous publication [12], that it is virtually impossible to distinguish between purely kinetic and thermodynamic factors as the dominant influence on either the initial formation or the thermal stability of the (metastable) tetragonal phase. Our result (see also [12]) that the first phase to form upon the crystallization of hydrous zirconia is the tetragonal polymorph is in agreement with the conclusion of many other investigators [14, 24, 35–39, 43, 48–50] (these investigators obtained the (metastable) tetragonal phase of zirconia either by precipitation from (aqueous) solutions followed by calcination or by thermal decomposition of zirconium salts). This observation appears to follow Ostwald's step rule: when a substance can exist in more than one modification, it is not the stablest polymorph with the lowest free energy which is formed first, but the least stable one, lying closest to the original state of free energy [51]. (Van Santen [51] has shown that the step rule could be related to the postulates of non-equilibrium thermodynamics, the multiple-step nature of the indirect process giving rise to a minimization of entropy production.) In view of this rationalization, it will be clear that structural similarities between the amorphous and tetragonal modifications of ZrO_2 are likely to be of paramount importance in the process of crystallization of the tetragonal phase from hydrous zirconia.

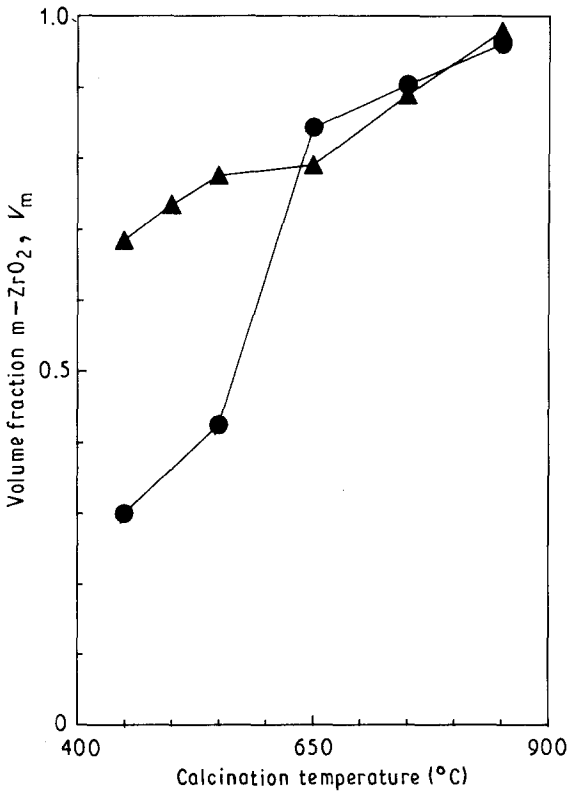

Figure 5 Effect of calcination temperature on the evolution of the volume fraction, V_m, of the monoclinic phase for the samples (●) ZrW and (▲) ZrE.

3.2.4. Tetragonal-to-monoclinic phase transformation

The (metastable) tetragonal-to-monoclinic phase transformation is also likely to be controlled by both thermodynamic (crystallite-size effects) and kinetic factors (nucleation kinetics) [12, 38, 52–54]. Purely crystallite-size effects can be discounted as explaining the promoting effect of ethanol washing on the process of phase transformation: the crystallite sizes obtained by X-ray line broadening and TEM analyses for the sample ZrE calcined at various temperatures up to 650 °C were smaller than or similar to those obtained for ZrW.

The nucleation of the monoclinic phase and the related kinetics of the phase transformation are likely to be influenced by impurities. As the crystallization and the subsequent phase transformations in the sample ZrE are preceded by the decomposition of surface ethoxide groups, we have carried out some preliminary experiments with the aim of examining whether carbonaceous impurities remaining from the decomposition were of influence on the rate of the (metastable) tetragonal-to-monoclinic phase transformation. To this end, two samples of xerogel of a freshly prepared batch of ZrE were heat treated at 450 °C for 15 h. One sample (designated ZrE1) was heat-treated (at a rate of 3 °C min^{-1}) in a flow of nitrogen (150 cm^3 min^{-1}), while the other (designated

ZrE2) was calcined in flowing air (150 $cm^3 min^{-1}$). The level of the carbonaceous residues in the sample ZrE1 (particularly, at the onset of the processes of crystallization and subsequent phase transformation to the monoclinic phase) was expected to be higher than in the sample ZrE2; this was affirmed by the colours of the two samples, that of ZrE1 being brown compared to the colour of ZrE2 which was white. (The amount of carbonaceous residues in the sample ZrE1 was estimated by TG-analysis to be approximately 2 wt%.) X-ray line broadening analyses showed that the crystallites of the two samples were similar in size (about 6.9–7.3 nm). On the other hand, X-ray phase analyses showed that the sample ZrE1 was to the extent of 90 vol% monoclinic zirconia, while the sample ZrE2 contained 76 vol% monoclinic phase. The phase composition of the sample ZrW (which has been washed only with water) was found to be independent of the nature of the flowing gas (nitrogen or air) used during heat treatment. Thus, the phase composition of the sample ZrE appears to be influenced by the presence and level of carbonaceous impurities, the (metastable) tetragonal-to-monoclinic phase transformation being promoted by carbonaceous residues.

We therefore conclude that post-precipitation washing with ethanol exerts little influence on the process of crystallization of hydrous zirconia: neither the temperature of crystallization nor the enthalpy change associated with the transition of the amorphous to the (metastable) tetragonal phase of zirconium dioxide were significantly influenced by the interaction between ethanol and hydrous zirconia during washing. On the other hand, the thermal stability of the tetragonal phase formed was found to be reduced drastically by effects imparted by the nature of the solvent used for washing the hydrogel; the process of phase-transformation to the thermodynamically more stable monoclinic modification was promoted strongly as a consequence of the washing with ethanol. This influence of ethanol-washing appears to arise from a promotional effect of carbonaceous residues. The carbonaceous impurities are thought to facilitate the nucleation of the monoclinic phase.

3.3. Influence of ethanol washing on the textural properties of zirconia

Full nitrogen adsorption–desorption isotherms were measured for granules of the samples ZrW and ZrE calcined at 450 °C; representative isotherms are shown in Fig. 6a. Both the isotherms were of type IV (BDDT classification [13, 55]), being characteristic of well developed mesoporous systems (pore radii between 1.0 and 25.0 nm). Following the classification of de Boer [56], the shape of the hysteresis loop in the isotherm measured on the sample ZrW was of type E while that exhibited by the sample ZrE showed more resemblance with the type A hysteresis loop. The pure type A hysteresis loop is characterized by adsorption and desorption branches which are almost vertical and nearly parallel over an appreciable range of gas uptake; such loops are often obtained with agglomerates of spheroidal particles of fairly uniform size and

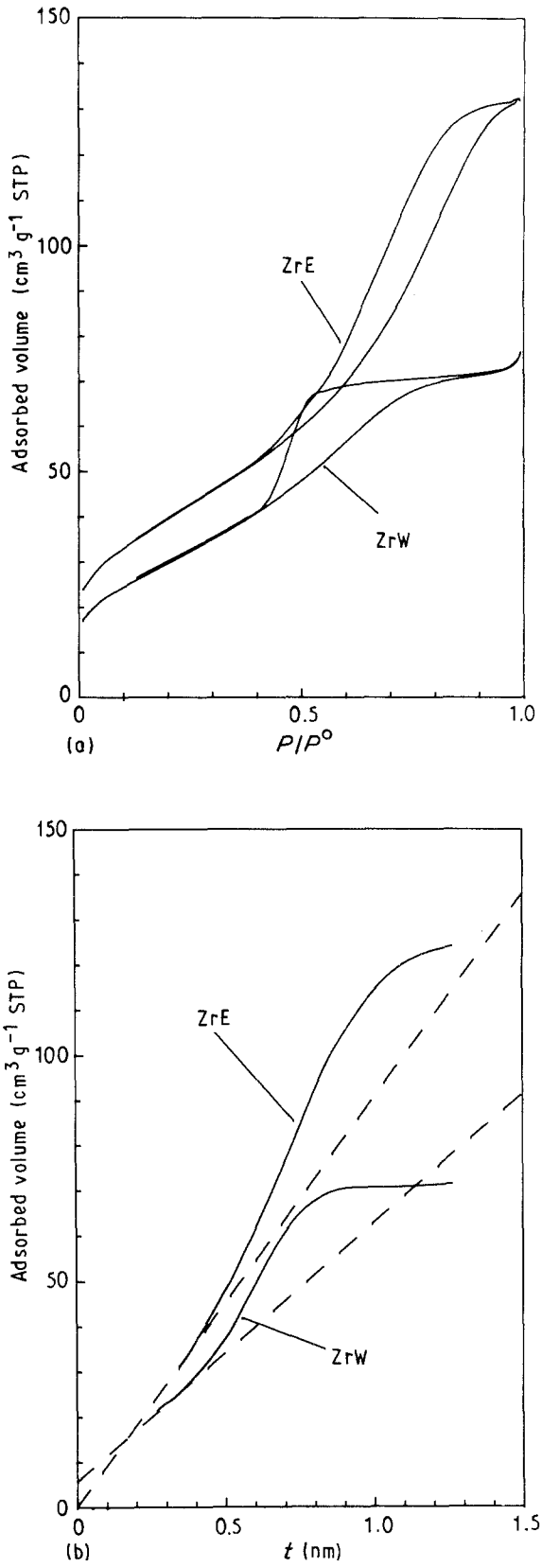

Figure 6 Results of nitrogen physisorption measurements performed on granules of the samples ZrW and ZrE which have been calcined at 450 °C. (a) Representative adsorption–desorption isotherms at −196 °C. (b) Typical V_{ads}–t plots obtained from analysis of the nitrogen adsorption data.

inter-particle coordination number [13, 55]. On the other hand, type E hysteresis is characteristic of porous solids which have a distribution of pores which would lead to type A hysteresis but for which the dimensions responsible for, in particular, the adsorption branch are heterogeneously distributed; e.g. there

are ink-bottle pores or voids between close-packed spherical particles [55, 56].

The most important textural parameters calculated from the isotherms are listed in Table I. The values of S_{BET} were calculated by the BET method by assuming a value of 0.162 nm^2 for the cross-sectional area of the nitrogen molecule [13, 55] and the total pore volumes, V_p, were calculated from the plateau of the corresponding adsorption isotherms [55]. The values of S_t (the sum of the areas of the mesopore walls and the external surface) were determined using the t-plot method [57]; examples of the plots of the adsorbed volume versus the statistical thickness, t, used in these calculations are shown in Fig. 6b. From this figure, it is also clear that whereas the linear branch of the t-plot of the sample ZrE extrapolated through the origin, that of ZrW showed a positive intercept on the adsorbed volume axis, this being indicative of the presence of microporosity (pores with radii not exceeding 1.0 nm) [55]; from the intercept and taking the appropriate density for liquid nitrogen [55], the numerical value for the micropore volume, V_{micro}, listed in Table I, was calculated. This result is consistent with the finding that the specific BET surface area of ZrW was significantly larger than the corresponding value of S_t; it is generally accepted that the presence of micropores leads to an over-estimation of the monolayer capacity and consequently to S_{BET} values which are unrealistically high [55]. The mesopore size distribution for each sample was calculated following the method developed by Barrett, Joyner and Halenda (the BJH method) assuming a cylindrical pore model [58]. The calculations were applied to the adsorption branch of the isotherms which, according to Broekhoff [59] and Everett [60, 61], is the stable branch when hysteresis loops of the type observed are involved. (Full details regarding these calculations have been given elsewhere [12].) The values of the most frequent pore radii, $R_p(max)^{ads}$, are listed in the last column of Table I. The corresponding pore size distributions are shown in Fig. 7.

From the results summarized in Table I, it is clear that post-precipitation washing with ethanol has a profound effect on the textural properties of (calcined) zirconium dioxide: the specific surface area, total specific pore volume and most frequent pore radius, were all increased significantly on washing with ethanol. Moreover, ethanol washing gave rise to a porous texture which was completely free of micropores. Results comparable with those given here for ZrO_2 have been reported by White *et al.* [62] who studied the effect of alcohol washing on the evolution of the surface area and porosity of alumina.

TABLE I Textural properties of ZrW and ZrE after calcination at 450 °C

Sample	S_{BET} ($m^2 g^{-1}$)	S_t ($m^2 g^{-1}$)	V_p ($cm^3 g^{-1}$)	V_{micro} ($cm^3 g^{-1}$)	$R_p(max)^{ads}$ (nm)
ZrW	111	89	0.11	0.010	2.1
ZrE	144	140	0.20	0	3.6

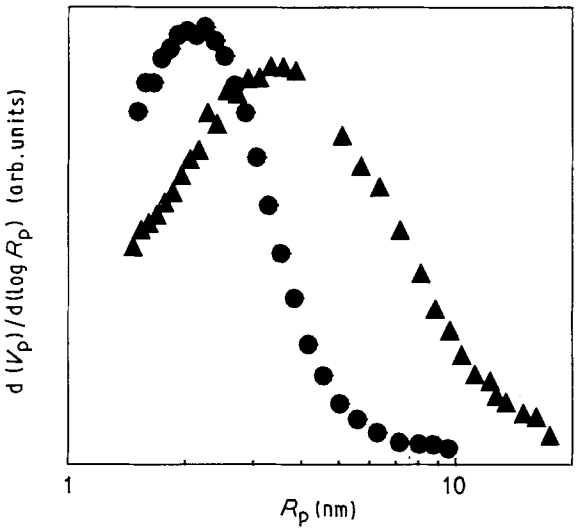

Figure 7 Representative mesopore size distributions for granules of the samples (●) ZrW and (▲) ZrE which have been calcined at 450 °C.

The effects of alcohol washing on the morphology and textural properties of zirconia and also of alumina have been rationalized in different ways. A number of investigators [19–21, 62] have attributed the effects to a reduction in capillary forces within the precipitate as a result of lowering the surface tension thus, leading to less pore collapse during the subsequent drying or calcination. In yet another approach, Readey *et al.* [63] explained the effects in terms of a steric inhibition between primary particles as a result of hydrogen bonding of ethanol to surface hydroxyl groups, thus inhibiting inter-particle polycondensation reactions which would lead to pore collapse and the formation of hard and dense agglomerates. Jones and Norman [22] showed that washing hydrous zirconia with methanol resulted in the removal of all non-bridging (terminal) hydroxyl groups and coordinated water; they proposed that it was this specific action of methanol (or, in general, of alcohols) which prevented inter-particle condensation reactions and thus also the formation of hard and dense agglomerates. More recently, Kaliszewski and Heuer [18] showed that surface ethoxide groups were formed during ethanol washing and postulated that the presence of these groups inhibited the inter-particle condensation reactions responsible for pore collapse and for the formation of hard agglomerates.

Purely surface tension effects can be discounted as explaining the effects of ethanol washing on the surface area and porosity of zirconia: preliminary experiments carried out in our laboratory, employing a range of different compositions of ethanol–water wash liquids (0, 25, 50 and 100 vol% ethanol–water), showed that any combination involving water in the wash liquid yielded xerogels which were of similar morphology (dense and glass-like) and texture (e.g. total specific pore volume) [64]; similar results were reported by White *et al.* [62] who investigated the interaction between alcohols and alumina precipitates. On the other hand, our results are consistent with those reported by Kaliszewski and Heuer [18], in that we also found unambiguous evidence that (surface)

ethoxide groups were formed during ethanol washing [30, 64]. Thus, in agreement with Readey *et al.* [63], with Jones and Norman [22], and with Kaliszewski and Heuer [18], we propose that the effects of ethanol washing (increase in specific surface area, pore volume and most frequent pore radius) derive from an inhibition of polycondensation reactions involving the surface hydroxyl groups located on adjacent particles which would have yielded new Zr–O–Zr bonds. The mechanism underlying this process of inhibition is believed to be associated with the formation of surface ethoxide groups.

4. Conclusions

1. Washing of the hydrogel of zirconia with ethanol was found to exert little influence on the process of crystallization of hydrous zirconia: neither the temperature of crystallization nor the enthalpy change associated with the transition of the amorphous to the (metastable) tetragonal phase of zirconia were significantly influenced.

2. The thermal stability of the tetragonal phase formed upon crystallization of hydrous zirconia was found to be reduced drastically by effects imparted by the nature of the post-precipitation washing liquid: the phase transformation to the thermodynamically more stable monoclinic phase was promoted strongly as a consequence of the washing with ethanol.

3. The effect of post-precipitation washing on the thermal stability of the (metastable) tetragonal phase appears to be related to the presence of carbonaceous residues on this material; these carbonaceous impurities are thought to facilitate the nucleation of the monoclinic phase of zirconia.

4. Post-precipitation washing with ethanol had a profound effect on the textural properties of (calcined) zirconia: the specific surface area, total specific pore volume and most frequent pore radius, were all increased significantly on washing the precipitate of zirconia with ethanol.

5. The effects of post-precipitation washing with ethanol on the textural properties of the ZrO_2 are probably due to an inhibition of polycondensation reactions of the surface hydroxyl groups located on adjacent particles which would have yielded new Zr–O–Zr bonds; this is probably associated with the presence of surface ethoxide species, the formation of which has been shown.

Acknowledgements

We thank W. Lengton for performing the wet-chemical analyses, H. Weber for his help with the XRF measurements, J. Boeijsma for his assistance with the X-ray powder diffraction measurements and R. Weierink for performing the FTIR and DRIFT measurements. Thanks are also due to Dr C. Otto, Faculty of Applied Physics, for his assistance in recording the laser Raman spectra. This research was partially financed by the Dutch Ministry of Economic Affairs (Innovative Research Programme on Catalysis).

References

1. H. FUJII, N. MIZUNO and M. MISONO, *Chem. Lett.* (1987) 2147.
2. L. A. BRUCE and J. F. MATHEWS, *Appl. Catal.* **4** (1982) 353.
3. L. A. BRUCE, G. J. HOPE and J. F. MATHEWS, *ibid.* **8** (1983) 349.
4. E. V. PROKHORENKO, N. V. PAVLENKO and G. I. GOLODETS, *Kinet. Catal.* (English Trans.) **29** (1988) 702.
5. J. G. van OMMEN, P. J. GELLINGS and J. R. H. ROSS, in "Methane Conversion", edited by D. M. Bibby, C. D. Chang, R. F. Howe and S. Yurchak (Elsevier, Amsterdam, 1988) p. 213.
6. K. C. PRATT, J. V. SANDERS and V. CHRISTOV, *J. Catal.* **124** (1990) 416.
7. J. P. van HOOK and J. C. YARZE, US Pat. 4026 823 (1977).
8. G. R. GAVALAS, C. PHICHITKUL and G. E. VOECKS, *J. Catal.* **88** (1984) 54.
9. K. TANABE, *Mater. Chem. Phys.* **13** (1985) 347.
10. D. L. TRIMM and A. STANISLAUS, *Appl. Catal.* **21** (1986) 215.
11. D. L. TRIMM, in "Design of Industrial Catalysts" (Chemical Engineering Monographs 11, Elsevier, Amsterdam, 1980).
12. P. D. L. MERCERA, J. G. van OMMEN, E. B. M. DOESBURG, A. J. BURGGRAAF and J. R. H. ROSS, *Appl. Catal.* **57** (1990) 127.
13. K. S. W. SING, D. H. EVERETT, R. A. W. HAUL, L. MOSCOU, R. A. PIEROTTI, J. ROUQUEROL and T. SIEMIENIEWSKA, *Pure Appl. Chem.* **57** (1985) 603.
14. H. TH. RIJNTEN, Thesis, Delft University of Technology (1971).
15. E. CRUCEAN and B. RAND, *Trans. Brit. Ceram. Soc.* **78** (1979) 58.
16. F. G. R. GIMBLETT, A. A. RAHMAN and K. S. W. SING, *J. Colloid Interface Sci.* **84** (1981) 337.
17. K. HABERKO, *Ceram. Int.* **5** (1979) 148.
18. M. S. KALISZEWSKI and A. H. HEUER, *J. Amer. Ceram. Soc.* **73** (1990) 1504.
19. R. YU. SHEINFAIN and T. F. MAKOVSKAYA, *Koll. Zh.* **38** (1976) 816.
20. A. ROOSEN and H. HAUSNER, in "Ceramic Powders", edited by P. Vincenzini, Materials Science Monographs 16 (Elsevier, Amsterdam, 1983) p. 773.
21. F. DOGAN and H. HAUSNER, in "Ceramic Transactions, Ceramic Powder Science II", Vol. 1, edited by G. L. Messing, E. R. Fuller Jr and H. Hausner (American Ceramic Society, Westerville, OH, 1988) p. 127.
22. S. L. JONES and C. J. NORMAN, *J. Amer. Ceram. Soc.* **71** (1988) C-190.
23. M. J. READEY, R. R. LEE, J. W. HALLORAN and A. H. HEUER, *ibid.* **73** (1990) 1499.
24. T. KOSMAC, R. GOPALA KRISHNAN, V. KRASEVEC and M. KOSMAC, *J. Phys. Coll. C1* **47** (1986) C1-43.
25. M. A. C. G. van de GRAAF, J. H. H. ter MAAT and A. J. BURGGRAAF, *J. Mater. Sci.* **20** (1985) 1407.
26. H. TORAYA, M. YOSHIMURA and S. SOMIYA, *J. Amer. Ceram. Soc.* **67** (1984) C-119.
27. P. D. L. MERCERA, J. G. van OMMEN, E. B. M. DOESBURG, A. J. BURGGRAAF and J. R. H. ROSS, *Appl. Catal.*, **78** (1991) 79.
28. R. SRINIVASAN, M. B. HARRIS, S. F. SIMPSON, R. J. De ANGELIS and B. H. DAVIS, *J. Mater. Res.* **3** (1988) 787.
29. M. J. TORRALVO, M. A. ALARIO and J. SORIA, *J. Catal.* **86** (1984) 473.
30. P. D. L. MERCERA, J. G. van OMMEN, E. B. M. DOESBURG, A. J. BURGGRAAF and J. R. H. ROSS, unpublished results 1988.
31. D. MICHEL, M. PEREZ y JORBA and R. COLLONGUES, *J. Raman Spectrosc.* **5** (1976) 163.
32. D. MICHEL, M. T. van den BORRE and A. ENNACIRI, in "Science and Technology of Zirconia III", edited by S. Somiya, N. Yamamoto and H. Yanagida, Advances in Ceramics Vol. **24** (1988) p. 555.
33. C. M. PHILLIPPI and K. S. MAZDIYASNI, *J. Amer. Ceram. Soc.* **54** (1971) 254.

34. V. G. KERAMIDAS and W. B. WHITE, *ibid.* **57** (1974) 22.
35. A. AYRAL, T. ASSIH, M. ABENOZA, J. PHALIPPOU, A. LECOMTE and A. DAUGER, *J. Mater. Sci.* **25** (1990) 1268.
36. J. LIVAGE, K. DOI and C. MAZIERES, *J. Amer. Ceram. Soc.* **51** (1968) 349.
37. F. C. WU and S. C. YU, *J. Mater. Sci.* **25** (1990) 970.
38. M. A. BLESA, A. J. G. MAROTO, S. I. PASSAGGIO, N. E. FIGLIOLIA and G. RIGOTTI, *ibid.* **20** (1985) 4601.
39. E. TANI, M. YOSHIMURA and S. SOMIYA *J. Amer. Ceram. Soc.* **66** (1983) 11.
40. R. CYPRES, R. WOLLAST and J. RAUCQ, *Ber. Deut. Keram. Ges.* **40** (1963) 527.
41. B. H. DAVIS, *J. Amer. Ceram. Soc.* **67** (1984) C-168.
42. R. SRINIVASAN, R. De ANGELIS and B. H. DAVIS, *J. Mater. Res.* **1** (1986) 583.
43. R. C. GARVIE, *J. Phys. Chem.* **69** (1965) 1238.
44. R. C. GARVIE and M. F. GOSS, *J. Mater. Sci.* **21** (1986) 1253.
45. R. C. GARVIE, *J. Phys. Chem.* **82** (1978) 218.
46. S. I. PYUN, H. J. JUNG and G. D. KIM, in "High Tech Ceramics", edited by P. Vincenzini (Elsevier, Amsterdam, 1987) p. 271.
47. T. MITSUHASHI, M. ICHIHARA and U. TATSUKE, *J. Am. Ceram. Soc.* **57** (1974) 97.
48. M. I. OSENDI, J. S. MOYA, C. J. SERNA and J. SORIA, *ibid.* **68** (1985) 135.
49. E. BERNSTEIN, M. G. BLANCHIN and A. SAMDI, *Ceram. Int.* **15** (1989) 337.
50. M. C. CARACOCHE, M. T. DOVA and A. R. LOPEZ GARCIA, *J. Mater. Res.* **5** (1990) 1940.
51. R. A. van SANTEN, *J. Phys. Chem.* **88** (1984) 5768.
52. R. P. DENKEWICZ Jr, K. S. TENHUISEN and J. H. ADAIR, *J. Mater. Res.* **5** (1990) 2698.
53. I. W. CHEN, Y. H. CHIAO and K. TSUZAKI, *Acta Metall.* **33** (1985) 1847.
54. A. H. HEUER, N. CLAUSSEN, W. M. KRIVEN and M. RUHLE, *J. Amer. Ceram. Soc.* **65** (1982) 642.
55. S. J. GREGG and K. S. W. SING, in "Adsorption, Surface Area and Porosity", 2nd Edn (Academic Press, London, 1982).
56. J. H. de BOER, in "The Structure and Properties of Porous Materials", edited by D. H. Everett and F. S. Stone (Butterworths, London, 1958) p. 68.
57. B. C. LIPPENS and J. H. de BOER, *J. Catal.* **4** (1965) 319.
58. E. P. BARRETT, L. G. JOYNER and P. P. HALENDA, *J. Amer. Chem. Soc.* **73** (1951) 373.
59. J. C. P. BROEKHOFF, in "Preparation of Catalysts II", edited by B. Delmon, P. Grange, P. Jacobs and G. Poncelet (Elsevier, Amsterdam, 1979) p. 663.
60. D. H. EVERETT, in "Characterization of Porous Solids", edited by K. K. Unger, J. Rouquerol, K. S. W. Sing and H. Kral (Elsevier, Amsterdam, 1988) p. 1.
61. D. H. EVERETT, in "Characterization of Porous Solids", edited by S. J. Gregg, K. S. W. Sing and H. F. Stoeckli (Society of the Chemistry Industry, London, 1979) p. 229.
62. A. WHITE, A. WALPOLE, Y. HUANG and D. L. TRIMM, *Appl. Catal.* **56** (1989) 187.
63. M. J. READEY, R. R. LEE and A. H. HEUER, in "89th Annual Meeting Abstracts" (American Ceramic Society, April 1987), p. 70-B-87.
64. P. D. L. MERCERA, R. B. G. VELTHUIS and J. R. H. ROSS, unpublished results 1991.

Received 9 May
and accepted 20 September 1991